6 Oxide Heterostructure Project (part I-II)

Project Leader: Hiroshi Kumigashira

6-1 Kinks in the Quasiparticle Band Dispersion of Perovskite Manganite $La_{0.6}S_{0.4}MnO_3$

The lack of information concerning many-body interactions in perovskite manganite $La_{0.6}S_{0.4}MnO_3$ (LSMO) has hindered our understanding the origin of unusual physical properties in the manganites. We have performed state-of-the-art *in situ* angle-resolved photoemission spectroscopy (ARPES) on LSMO to address the fine electronic structures near the Fermi level (E_F) and many-body interactions in quasiparticles. The kink structure indicative of the strong electron-boson coupling in LSMO is clearly observed near E_F. The momentum dependence of the kinks suggests that polaronic quasiparticles produced by the coupling of electrons with Jahn-Teller phonons play an essential role in the unusual physical properties of manganites.

$La_{0.6}S_{0.4}MnO_3$ (LSMO) is a typical hole-doped perovskite manganite that has attracted considerable attention because of its unusual physical properties, such as colossal magnetoresistance (CMR) behavior and the half-metallic nature of its ground state [1]. These remarkable properties originate from the complex interplay between the charge, lattice, orbital, and spin degrees of freedom [2]. In order to clarify the origin of these properties of LSMO, it is important to understand the interactions of electrons with various degrees of freedom. Angle-resolved photoemission spectroscopy (ARPES) is a powerful tool for investigating many-body interactions in quasiparticles as functions of binding energy and momentum. From the line-shape analysis of the ARPES spectra, the momentum-resolved self-energy of quasiparticles, which reflects many-body interactions, has been widely examined in strongly correlated electron systems, most notably in the high-T_c cuprate superconductors [3].

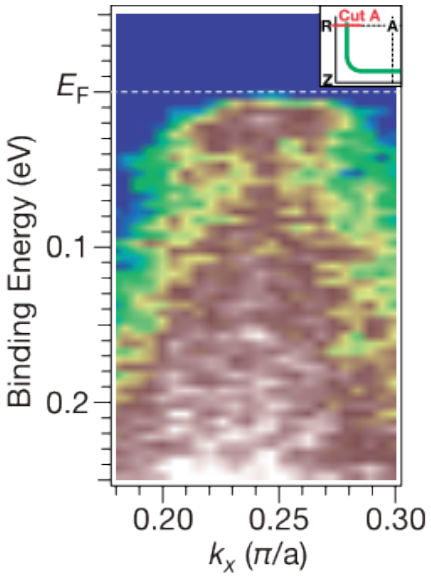

Fig. 1: ARPES intensity map for the hole band of LSMO films along the *R–A* direction (cut A in the inset) in the near-E_F region. The inset shows the illustration of the hole FS.

However, so far, there has been not any report on the observation of low-energy excitations near the Fermi level (E_F) in LSMO despite of intensive ARPES investigations [4, 5]. The lack of information concerning many-body interactions in the electronic structure near E_F has hindered our understanding the origin of unusual physical properties in manganites. Thus, in order to examine the fine structure appearing near E_F as a result of many-body interactions, we have performed state-of-the-art *in situ* ARPES measurements on high-quality LSMO films grown by laser molecular beam epitaxy, and succeeded in observing the kink structure near E_F in the quasiparticle band dispersion [6].

Figure 1 show the ARPES intensity plot of the hole band dispersion along the *R-A* direction of LSMO (cut A in the inset). We clearly observed the remarkable intensity modulation in the band structure near E_F, which corresponds to the

"peak-dip-hump" structure in ARPES spectra (not shown) derived from the quasiparticle excitation [3]. In order to examine the possible coupling of quasiparticles with collective excitations from the aspect of its energy scale and strength, we analyzed the momentum distribution curves (MDCs) of the ARPES spectra. Fig. 2(a) shows the band dispersion determined by plotting the peak positions of MDCs for the ARPES data shown in Fig. 1. A clear kink in the band dispersion is observed at the binding energy of approximately 50 meV.

Whether or not the observed kink shows momentum dependence is a next crucial issue for identification of relevant many-body interactions. Figures 2(a)-(e) show the band dispersions along cuts A–E for the hole Fermi surface [see Fig. 2(f)]. The clear kinks around 50 meV are observed throughout the hole FS, indicating the isotropic nature of the kink. Furthermore, the detailed analysis revealed that the kinks have almost the same coupling strength: As summarized in Fig. 2(g), the strength of the electron-boson coupling, which is estimated from the ratio between the Fermi velocity v_F and the bare-band velocity v_b, is constant for all the band dispersions of the hole FS (v_b/v_F = 2.5–3). The observed isotropic behavior of kinks is most likely caused by localized bosons coupled with electrons. In connection with the previously reported inelastic neutron scattering results [7], it is reasonable to conclude that the kink results from the interaction of electrons with Jahn-Teller (JT) phonon modes. Strong interaction between electrons and local JT phonons in LSMO has been considered to lead to the formation of JT small polarons. Thus, these results suggest that the polaronic quasiparticles play an important role in the CMR behavior of the ferromagnetic metallic phase of LSMO. Our findings will contribute to understanding the unusual physical properties of manganites with regard to the origin of CMR phenomena.

6-2 Close relationship between the two characteristic features of metallic quantum well states in $SrVO_3$ ultrathin films

Metallic quantum well (QW) structures based on transition metal oxides provide a platform for studying the behavior of strongly correlated electrons under quantum confinement. Metallic QW states observed in $SrVO_3$ ultrathin films show two distinctive features that have not been observed in conventional metallic QW, i.e., orbital-selective quantization and anomalous subband-dependent mass enhancement. Here, we report the existence of a close relationship between the two characteristic features in terms of *in-situ* angle resolved photoemission spectroscopy (ARPES) measurements and detailed line-shape analysis of ARPES spectra.

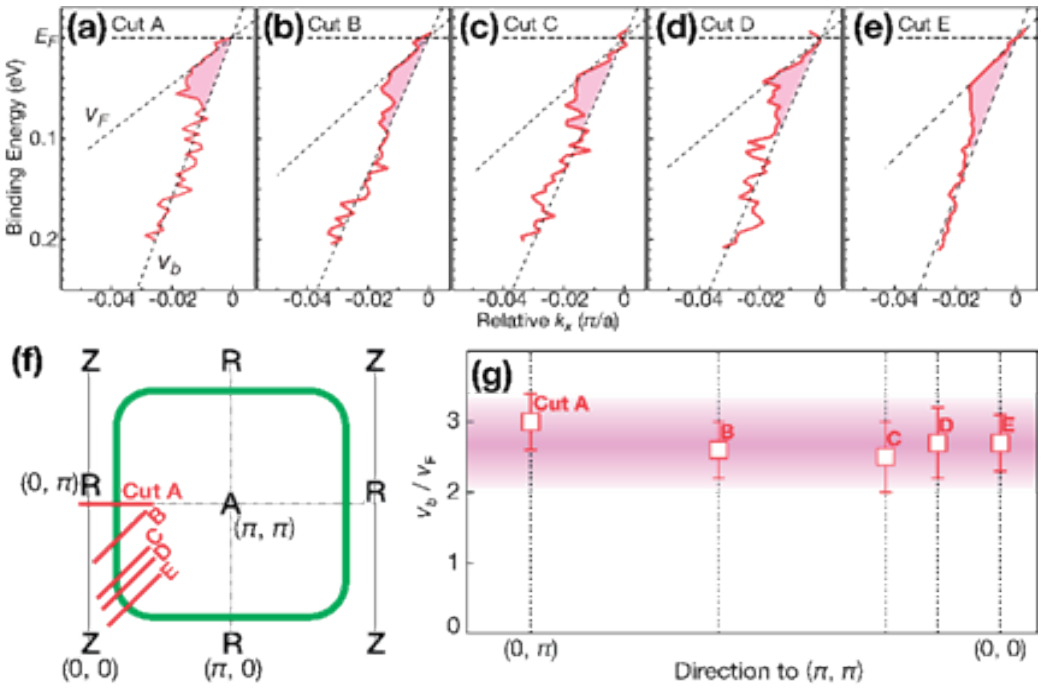

Fig. 2: (a)–(e) Band dispersions obtained from MDCs along cuts A–E, respectively, in (f). (f) The illustration of the hole Fermi surface in LSMO, together with the measurement cuts. (g) The values of v_b/v_F obtained from linear fitting of the band dispersion along cuts A–E.

Quantum confinement of strongly correlated electrons in oxide heterostructures has attracted much interest for not only its promising technological applications in future oxide electronics [8], but also understanding the fundamental low-dimensional physics of strongly correlated electron systems [9]. Recently, metallic quantum well (QW) states have been discovered in $SrVO_3$ (SVO) ultrathin films grown on Nb:$SrTiO_3$(001) substrates [10]. The observed QW states exhibit two distinctive features. The first is *orbital-selective quantization* originating from the anisotropic orbital character of the V 3*d* t_{2g} (d_{xy}, d_{yz}, and d_{zx}) band states, as shown in Fig. 3(a). Each orbital essentially has a two-dimensional (2D) character in the respective plane. Consequently, the d_{yz}/d_{zx} bands are subject to quantization [from 2D to one-dimensional (1D)], while the d_{xy} band remains unchanged (maintaining its 2D character). The other characteristic behavior is *anomalous subband-dependent mass enhancement*: the subband dispersion becomes considerably narrower as its bottom energy (quantization energy) E_n approaches the Fermi level (E_F) [see Fig. 3(b)]. Such anomalous mass enhancement (narrowing) in subbands has not been observed in the conventional metallic QW structure based on metals having nearly free-electron-like *sp* states [11]. Therefore, the anomalous mass enhancement, as well as the orbital selective quantization, is a characteristic behavior of confined strongly correlated electrons. Despite intense theoretical and experimental studies, however, the physical origin is not yet understood. To address this issue, we have performed *in-situ* angle-resolved photoemission spectroscopy (ARPES) measurements on SVO ultrathin films and analyzed the line shape of ARPES spectra, particularly focusing on the width of momentum distribution curves (MDCs) [12].

Figure 3(b) shows the dispersion of each subband $\varepsilon_n(\boldsymbol{k})$ determined from the ARPES measurements, together with the MDC at E_F. It is evident that the MDC width Δk becomes wider with increasing quantum number n for each film thickness and as E_n approaches E_F. From a Δk value, one can estimate the imaginary part of self-energy ImΣ reflecting electron-electron correlation [13]. The obtained ImΣ values for each subband are plotted in Figs. 4(a)–(c) as a function of binding energy ω. As can be seen, the rate of increase of Im$\Sigma(\omega)$ tends to be larger with increasing n and/or decreasing thickness, namely as E_n approaches E_F.

In order to evaluate the strength of electron correlation, Im$\Sigma(\omega)$ curves are fitted to the following equation, which assumes the Fermi liquid ground state [12]:

$$\left|Z_n \mathrm{Im}\sum(\omega)\right| = \Gamma_n^{\mathrm{imp}} + \beta_n(\omega^2 + (\pi k_B T)^2) \qquad (1)$$

where β_n denotes a coefficient reflecting the strength of electron correlation, k_B is the Boltzmann constant, and Γ_n^{imp} is the inverse lifetime of quasiparticles associated with the impurity scattering. The curve fitting well reproduces the experimental results, as shown in Figs. 4(a)–(c). The estimated β_n is plotted against E_n in Fig. 4(d). As E_n approaches E_F, the value of β_n is

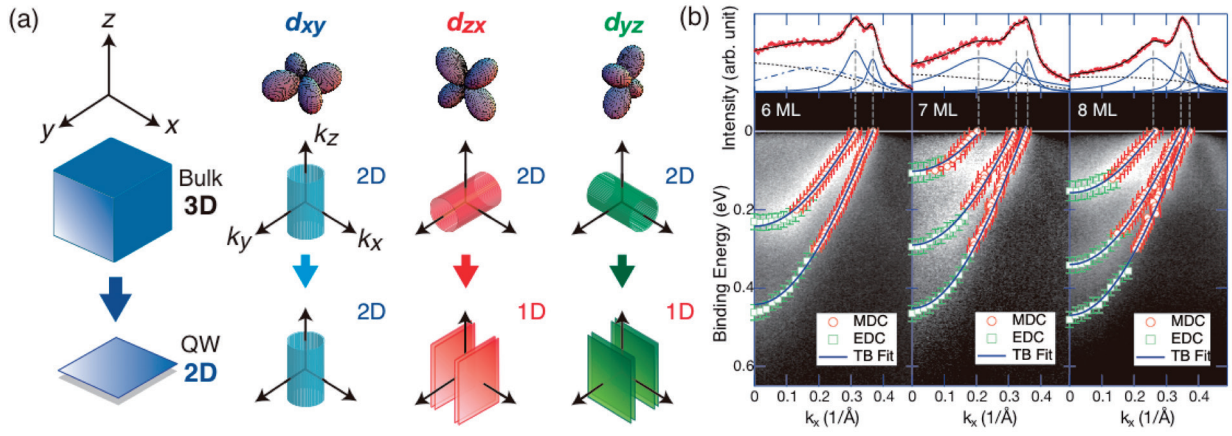

Fig. 3: Quantum well states in $SrVO_3$ ultrathin films. (a) Schematic illustration of the QW structure and quantization of V-3*d*-derived states. Owing to the 2D character of each orbital in the respective plane, the d_{yz}/d_{zx}-derived electronic structures are subject to quantization (from 2D to 1D), while that of the d_{xy} orbital remains unchanged (from 2D to 2D). (b) ARPES intensity plots for d_{zx} subbands of 6-ML, 7-ML, and 8-ML $SrVO_3$. The top panels show the corresponding MDCs at E_F.

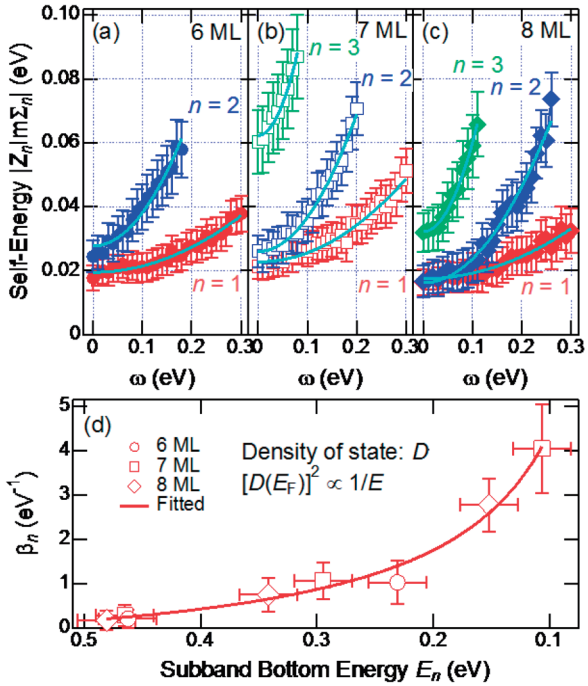

Fig. 4: Self-energy for $SrVO_3$ QW states. (a)–(c) $Im\Sigma_n$ of each subband plotted as a function of ω for 6-, 7-, and 8-ML $SrVO_3$ ultrathin films. (d) E_n dependence of β_n estimated from the curve fit. The solid curve is the result of fitting assuming the quasi-1D DOS.

considerably enhanced, indicating that the electron correlation significantly contributes to the anomalous subband-dependent mass enhancement in SVO QW states.

The trend of the observed enhancement of electron correlation seems to be opposite to what would be expected from the Fermi-liquid behavior. In general, the strength of the electron-electron interaction is proportional to the square of the density of state (DOS) D at E_F. Therefore, based on the behavior of bulk SVO [14], a weaker correlation effect is expected in the subbands located at lower binding energies owing to the reduction of band filling [15]. The seeming contradiction can be reconciled by considering the orbital-selective quantization as shown in Fig. 3(a): in the present case, the quasi-1D electronic states are realized in the d_{yz}/d_{zx}-derived subbands by the further dimensionality reduction (from 2D to 1D) due to the quantum confinement. DOS in 1D systems is proportional to $1/\sqrt{E}$, where E is the energy measured from the band edge. Thus, the β_n within the quasi-1D d_{yz}/d_{zx} subbands will be proportional to $[D(E_F)]^2 \propto 1/E_n$, which is the opposite behavior of the three-dimensional case ($[D(E_F)]^2 \propto E_n$). Indeed, the experimental results are adequately reproduced by the curve fit assuming the quasi-1D state as shown in Fig. 4(d).

These results indicate the close relationship between the two characteristic behaviors of metallic QW states in $SrVO_3$ ultrathin films: the *anomalous subband-dependent mass enhancement* originates from the quasi-1D nature of the quantized V 3*d* states as a result of the *orbital-selective quantization*. The present study demonstrates that the QW structure of strongly correlated oxide will provide an ideal platform for both investigating the behavior of correlated electrons and for manipulating novel quantum phenomena in reduced dimensions.

BEAMLINE

28A and 2A

BL-2A and 28A

References

[1] Colossal Magnetoresistive Oxides, edited by Y. Tokura, Advances in Condensed Matter Science Vol. **2** (Gordon and Breach, Amsterdam, 2000).
[2] M. Imada, A. Fujimori, and Y. Tokura, Rev. Mod. **70**, 1039 (1998).
[3] A. Damascelli, Z. Hussain, and Z.-X. Shen, Rev. Mod. Phys. **75**, 473 (2003).
[4] A. Chikamatsu et al., Phys. Rev. B **73**, 195105 (2006).
[5] L. L. Lev et al., Phys. Rev. Lett. **114**, 237601 (2015).
[6] K. Horiba et al., Phys. Rev. Lett. **116**, 076401 (2016).
[7] W. Reichardt and M. Braden, Physica B **263-264**, 416 (1999).
[8] H. Y. Hwang et al., Nat. Mater. **11**, 103 (2012).
[9] M. Imada, A. Fujimori, and Y. Tokura, Rev. Mod. Phys. **70**, 1039 (1998).
[10] K. Yoshimatsu et al., Science **333**, 319 (2011).
[11] I. Matsuda et al., Phys. Rev. B **65**, 085327 (2002).
[12] M. Kobayashi et al., Phys. Rev. Lett. **115**, 076802 (2015).
[13] T. Valla et al., Science **285**, 2110 (1999).
[14] I. H. Inoue et al., Phys. Rev. B **58**, 4372 (1998).
[15] W. F. Brinkman and T. M. Rice, Phys. Rev. B **2**, 4302 (1970).